Composites: Part B 54 (2013) 20–27

Contents lists available at SciVerse ScienceDirect

Composites: Part B

journal homepage: www.elsevier.com/locate/compositesb

Subcritical damage mechanisms of bolted joints in CFRP composite laminates

A. Ataş [a,*], C. Soutis [b]

[a] Department of Mechanical Engineering, Balikesir University, Balikesir 10145, Turkey
[b] Faculty of Engineering and Physical Sciences, University of Manchester, Manchester M13 9PL, UK

ARTICLE INFO

Article history:
Received 3 January 2013
Received in revised form 8 April 2013
Accepted 18 April 2013
Available online 3 May 2013

Keywords:
A. Polymer–matrix composites (PMCs)
D. Mechanical testing
D. Radiography
E. Joints/joining
Subcritical damage mechanisms

ABSTRACT

A detailed experimental programme is presented that was conducted in order to establish a data base for strength and subcritical damage mechanisms of bolted joints in CFRP composite laminates. Single fastener double-shear tensile tests for various joint geometries were performed for a range of cross-ply and quasi-isotropic lay-ups of HTS40/977-2 CFRP material system. Penetrant enhanced X-ray radiography was used to define the subcritical damage locations which are of great importance when modelling the failure response of the joints. It is suggested that the subcritical damage planes can be modelled using cohesive zone elements (CZEs) in order to develop physically based strength prediction methods for bolted joints in CFRP laminates.

1. Introduction

The primary reasons for the high demand in carbon fibre reinforced plastic (CFRP) composites are their outstanding specific stiffness and strength properties, which in turn lead to substantial weight reductions. These advantages, however, may not be fully utilised unless the structural joints are designed efficiently since the joint efficiency of ductile metals has been shown to be as much as twice that of the CFRP composites [1–4]. This high efficiency of the metallic materials is based on their extensive yielding capability. Composite laminates also show some stress concentration relief, although each of its constituents (the resin matrix and fibres) behaves in a brittle manner up to failure. Subcritical damage modes such as transverse matrix cracks, axial splits (fibre/matrix shearing) and delaminations between adjacent layers around the highly stressed regions of the hole boundary contribute to that stress concentration relief. Most of the strength prediction techniques to date (characteristic curve, stress concentration reduction factor, progressive failure analysis) rely on some form of empirical correlation factors in order to take these subcritical damage modes into account. These correlation factors are usually functions of the material system, joint geometry, clamping torque, laminate lay-up and stacking sequence. The aim of the present work was to identify the locations of the subcritical damage mechanisms, as well as joint strengths, for various joint geometries and laminate lay-ups using the penetrant enhanced X-ray radiography technique. Those critical locations provide significant information and physical understanding leading to eliminate the need for the experimental correlation factors in order to develop consistent strength prediction techniques.

2. Material system and specimen design

The material system used in this study is HTS40/977-2 carbon fibre–epoxy in the form of pre-impregnated (prepreg) tape. The prepreg tapes were made of unidirectional high tensile strength/standard modulus aerospace grade carbon fibres (Toho Tenax®, HTS40-F13-12K-800tex) pre-impregnated with 177 °C curing toughened epoxy resin (Cycom®9770-2). The nominal thickness of the prepreg tape is 0.25 mm with a fibre volume fraction of 58% [5].

The composite laminates were fabricated by the hand lay-up technique in an autoclave according to the manufacturer's recommended curing procedure. A diamond tip saw was used to cut the laminates to dimensions with special care given to the precise alignment of the laminates. Fastener holes were drilled with a backing plate in order to prevent drilling induced delamination failure. The laminates were inspected by X-ray radiography to establish specimen quality. For more information on the experimental programme, refer to Ref. [4].

Typical specimen geometry of a pin joint in a composite laminate is shown in Fig. 1 with definitions of the width (w), free edge distance (e), hole diameter (d) and thickness (t). The x–y and 1–2

* Corresponding author. Tel.: +90 266 6121194; fax: +90 266 6121257.
E-mail address: a.atas@balikesir.edu.tr (A. Ataş).

1359-8368/$ - see front matter © 2013 Elsevier Ltd. All rights reserved.
http://dx.doi.org/10.1016/j.compositesb.2013.04.071

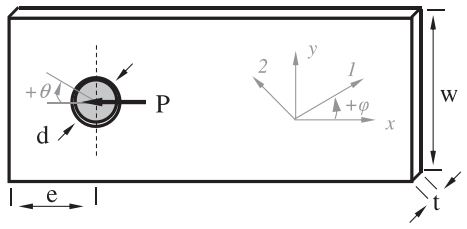

Fig. 1. Geometrical definitions of a pin joint in a composite laminate.

coordinate systems define the global laminate and local material coordinate systems, respectively. The angle φ defines the layer orientation angle with respect to the x (loading) axis and the angle θ defines the circumferential co-ordinate direction around the hole boundary. Double-lap pin and bolted joint loading fixtures were manufactured in accordance with the ASTM standard D5961/D5961M-01 [6]. Stainless steel pins of 5.98 mm and 12.9 grade steel bolts of 5.95 mm diameter were used to load the pin and bolted joint specimens, respectively.

Failure of a mechanical joint describes failure of the fastener hole in this study and stress concentrations around the fastener hole under applied loads are the primary reason for the failure of a joint. Net-tension, shear-out and bearing are three common in-plane failure modes observed in single pin joints in CFRP composite laminates [7–9]. These failure modes can be developed in isolation or in combination to each other depending upon various factors which may affect the stress distributions and thus, the mode of failure. Specimen geometrical ratios such as w/d and e/d (see Fig. 1), laminate lay-up and material system are the most important parameters among others [3,7–13]. Typical in-plane critical stress distributions around a pin-loaded hole are the normal stresses at the net-tension plane, shear stresses at the shear-out plane and the radial bearing stresses at the bearing plane as illustrated in Fig. 2. The stresses decay rapidly away from the hole boundary at the net-tension and shear-out planes with increased w and e respectively, and maximum radial compression (bearing) stress develops at the bearing plane due to the fastener/hole interaction.

In the geometrical aspect, net-tension mode is observed when the specimen width is not wide enough to relieve the high normal stress gradients (low w/d ratio). Shear-out mode is observed in laminates with adequate width against the net-tension mode but insufficient free edge distance to relieve the high shear stresses developed at the shear-out plane (low e/d ratio). In the net-tension and shear-out failure modes, the compressive stresses developed at the bearing plane are not high enough to cause significant fibre failure before those net-tension or shear-out modes occur. Bearing mode is caused by the compressive stresses and includes matrix cracking, fibre microbuckling and kinking with a significant amount of delamination.

3. Measurement of joint strength and determination of damage locations

Tests were conducted at room temperature with a Hounsfield electromechanical testing machine at a 1 mm/min loading rate. Applied load and the cross-head displacement were recorded by a computer aided data acquisition system [4]. Tests were stopped after a significant (approximately 30%) load drop was observed in the load–displacement curve, according to ASTM standard [6]. Finger-tight bolted joints were chosen according to standard design practices where the fully-tightened joints are assumed to be loosened due to service loading conditions.

After testing, the specimens were inspected using penetrant enhanced X-ray radiography with a Hewlett Packard Model 43855-A X-ray machine. This is a widely used and well established non-destructive testing technique for composite materials [8,14–16]. The technique is based on the variations of X-ray absorption through the thickness of the laminate due to the presence of defects such as matrix cracks, fibre splitting and delamination. An X-ray opaque penetrant solution is generally applied to the area of interest, which penetrates into the defects, in order to obtain adequate contrast. This technique is especially suited for inspections around the boundaries, such as free edges or fastener holes, because of the ease of application of the penetrant fluid through the boundary. However, it must be noted that if a defect is closed or surrounded by undamaged material, then it would not be possible to observe it by the X-ray technique.

3.1. Cross-ply specimens

Cross-ply specimens are often not used in real life structural applications. They were used in this work, however, due to their relatively apparent damage locations to facilitate comparison with

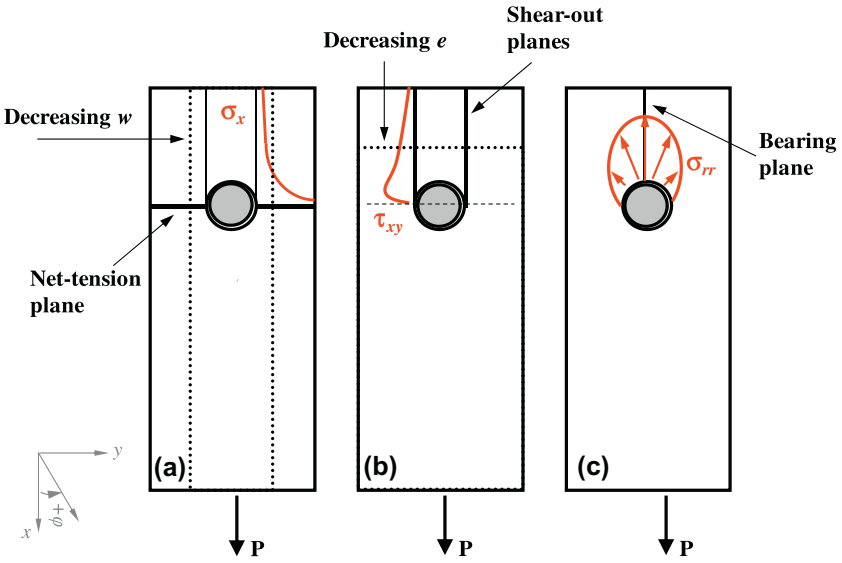

Fig. 2. Influence of geometrical parameters on the failure of pin joints.

Table 1
Cross-ply pin and finger-tight bolted joint specimen test parameters.

Laminate pattern	Specimen code	w/d	e/d
$[90°/0°]_s$	P1W (Pin)	6	3
	B1W (Bolt)	6	3
$[90^\circ_2/0^\circ_2]_s$	P2W (Pin)	6	3
	B2W (Bolt)	6	3
$[90°/0°]_{2s}$	B3W (Bolt)	6	3
	B3N (Bolt)	3	3

the FE predictions. Three cross-ply lay-ups, as shown in Table 1, were tested considering the effect of sublaminate-level ($[90°/0°]_{2s}$) and ply-level ($[90^\circ_2/0^\circ_2]_s$) scaled laminates on the bolted joint strength [17–20]. (*W* and *N* stand for the wide and narrow specimens, respectively). Laminates with 90° outer layers were used to provide the same degree of constraint for the inner 0° layers [21]. The width-to-hole diameter and edge distance-to-hole diameter ratios were kept constant ($w/d = 6$ and $e/d = 3$ for $d = 6$ mm) for most joint configurations. For selected $[90°/0°]_{2s}$ lay-up the $w/d = 3$ ratio was also used to observe any failure mode and strength dependency on the specimen geometry. Typical load–displacement curves of the $[90°/0°]_s$ lay-up specimens are shown in Fig. 3.

The pin joints in $[90°/0°]_s$ lay-up initially exhibit predominantly linear behaviour. This is followed by a nonlinear portion with a considerable stiffness loss and consequently a sudden load drop due to the extensive bending of the laminate under compressive pin contact stresses without any lateral support. Finger-tight lateral support prevents the sudden failure of the $[90°/0°]_s$ lay-up and provides a strength increase of 16% [4]. Similar results were reported by Smith and Pascoe [22] for the $[0°/90°]_s$ lay-up. (The bolted joint appears softer in Fig. 3 due to some slippage that occurred during the tests).

The X-ray images of pin (P1W) and finger-tight bolted (B1W) joints in $[90°/0°]_s$ lay-up are shown in Fig. 4i and ii, respectively. Transverse matrix cracks, compressive fibre failure and delamination damage are observed in the pin joint specimens. The local fibre compressive failure initiated at the highly loaded bearing area (indicated by arrow *d* in Fig. 4i) and it triggered delamination between the 90° and 0° layers. Increased loading, following the delamination, caused excessive bending of the layers and resulted in a sudden load drop in the load–displacement curve, as shown in Fig. 3. This extensive local damage prevented the development of any axial splitting due to increased pin displacement.

The finger-tight lateral constraint changed the damage mechanisms drastically as shown in Fig. 4ii. Axial splits running from the hole edge (approximately tangent to $\theta = 90°$) to the free edge were observed in addition to failure modes observed in the pin joints. The washers prevented any premature bending of the layers due to the local fibre compression failure. The increased bolt displacement caused the groups of 0° layers to be sheared-out after delaminating from the 90° layers as reported by Hart-Smith [3]. These splits were accompanied by widespread 90° transverse matrix cracks.

The characteristic "V" shape of the fibre compressive failure observed in almost all cross-ply lay-ups by X-ray radiography is similar to that of 0° laminates (transversely constrained from splitting) reported by Collings [23] as shown in Fig. 5i. This is a fibre instability failure mode, observed also in open hole specimens loaded in compression as shown in Fig 5ii, that initiates due to local fibre buckling and propagates across the specimen width, forming a kink band zone (fibre kinking) [5,15,24].

The load drop is more gradual for the pin joints of relatively thicker ply-level scaled $[90^\circ_2/0^\circ_2]_s$ lay-up as shown in Fig. 6. This is probably due to the increased bending stiffness of the central 0° layers which allows more progressive damage to occur before

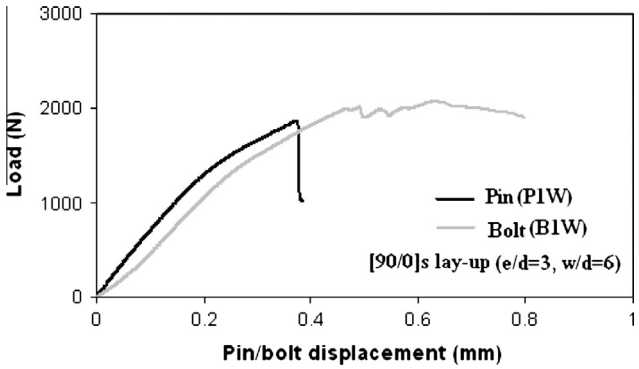

Fig. 3. Typical load–displacement curves of pin and finger-tight bolted joints in $[90°/0°]_s$ lay-up ($e/d = 3$, $w/d = 6$).

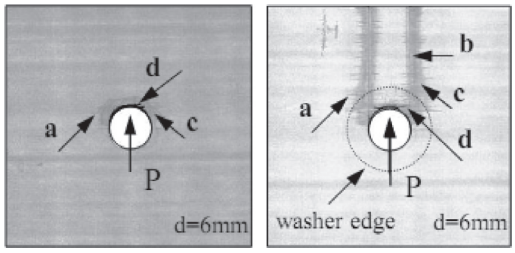

Fig. 4. X-ray radiographs showing damage in pin and finger-tight bolted joints in $[90°/0°]_s$ lay-up at failure: (a) transverse matrix cracks, (b) axial splitting, (c) delamination, and (d) compressive fibre failure in 0° layers.

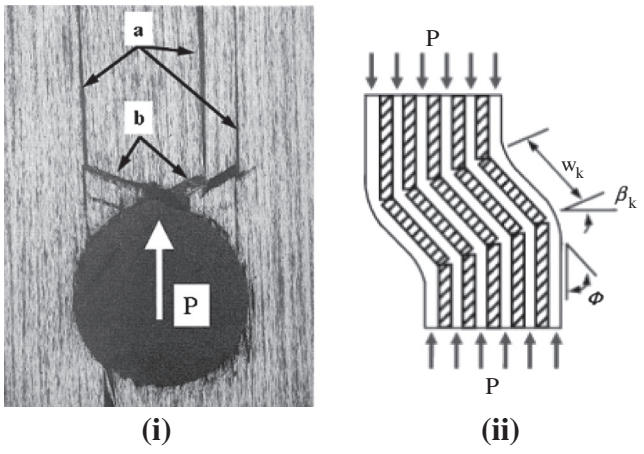

Fig. 5. (i) Bearing failure in a laterally constrained [0°] laminate: (a) axial splitting, (b) compressive fibre failure (hole diameter is 6.35 mm) [23], and (ii) formation of kink band zone (w_k: kink band width, β_k: boundary orientation and Φ: inclination angle) [5].

any catastrophic bending of the layers. It is clear from the X-ray radiograph in Fig. 7i that some degree of splitting develops. However, eventual bending (out-of-plane deflection) of the central 0° layers, accompanied with extensive delamination, causes final failure before the splits reach the free edge.

The finger-tight washers limited the bending of the 0° layers which resulted in less delamination damage that was similar to that observed for the $[90°/0°]_s$ lay-up. Consequently the splits that were accompanied by extensive transverse matrix cracks grew to the free edge with increased bolt displacement as seen in Fig. 7ii.

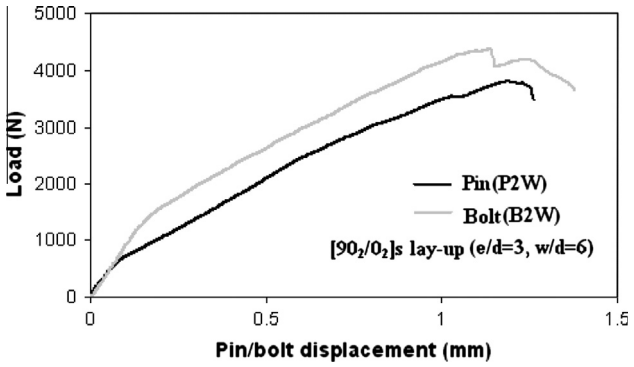

Fig. 6. Typical load–displacement curves of pin and finger-tight bolted joints in $[90^{\circ}_2/0^{\circ}_2]_s$ lay-up ($e/d = 3$, $w/d = 6$).

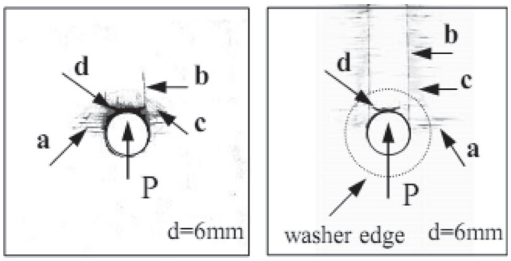

Fig. 7. X-ray radiographs showing damage in pin and finger-tight bolted $[90^{\circ}_2/0^{\circ}_2]_s$ lay-up at failure load: (a) transverse matrix cracks, (b) axial splitting, (c) delamination, and (d) compressive fibre failure in 0° layers.

The bearing strength of the cross-ply specimens (S_{max}) at failure are given in Fig. 8. The bearing strength is defined as:

$$S_{max} = P_{max}/dt \quad (1)$$

where P_{max} is the maximum load sustained by the joint, d and t are the hole diameter and laminate thickness, respectively.

The increased thickness reduced the coefficient of variation (C_v) in the pin joints due to the increased specimen stability, as explained earlier, without a significant strength increase. Comparison of X-ray radiographs, Figs. 4i and 7i, clearly shows that the thinner $[90^{\circ}/0^{\circ}]_s$ lay-up experienced much less local damage than the thicker $[90^{\circ}_2/0^{\circ}_2]_s$ lay-up due to the premature bending of the material beneath the pin. Any physical comparison regarding the failure mechanisms will therefore not be reasonable for the pin joints.

For the bolted joints, the sublaminate-level scaled $[90^{\circ}/0^{\circ}]_{2s}$ lay-up showed a strength increase of approximately 19% over the $[90^{\circ}/0^{\circ}]_s$ lay-up whereas the ply-level scaled $[90^{\circ}_2/0^{\circ}_2]_s$ lay-up only showed a 4% strength increase. The significant strength increase of sublaminate-level scaled specimens is due to the interspersion of the layers instead of grouping them together as in ply-level scaled specimens.

The key features of the global shear-out failure mode observed in the bolted joints of cross-ply laminates are the splitting within the 0° layers and the delaminations between the consecutive layers. Grouping the layers together has a twofold effect on the strength of those joints. First, the splits initiate at the hole edge and grow through-the-thickness of the grouped layers without an interruption from the adjacent layers. Second, grouping the layers reduces the number of the interfaces and therefore increases the magnitude of the shear stress to be carried by each interface [25]. As a result, greater delamination was developed under lower load levels for the ply-level scaled $[90^{\circ}_2/0^{\circ}_2]_s$ lay-up with a broader extent of transverse matrix cracks. Although this could result in a stronger joint in a quasi- or near quasi-isotropic lay-up that fails in net-tension mode by providing better stress concentration relief [2], that greater delamination size has facilitated the shear-out mode for the cross-ply lay-up due to poorer shear properties.

Fig. 9 shows the schematic of the subcritical in-plane damage planes observed from the X-ray radiographs of the cross-ply lay-ups. The extent of the transverse matrix cracks dispersed along the axial splits as shown in X-ray radiographs. However, it has been shown that those transverse matrix cracks can be represented as a single crack where the maximum stress concentration occurs for the centre notched specimens [26]. Thus, based on this assumption, transverse matrix cracks were characterised as single cracks at the maximum stress concentration locations ($\theta = \pm 90^{\circ}$). Axial split planes within the 0° layers were extended from the hole edge at $\theta = \pm 90^{\circ}$ to the free edge as observed from the radiographs.

3.2. Quasi-isotropic specimens

Bolted joints of three different quasi-isotropic laminates of practical interest, designated as Q1, Q2 and Q3, were tested with varied w/d ratio ($e/d = 3$, $d = 6$ mm) as shown in Table 2. (W and N stand for the wide and narrow specimens, respectively).

Typical load–displacement curves of the Q1 specimens as a function of w/d are shown in Fig. 10. Both curves show almost identical characteristics. Bearing was the global mode of failure for both joints, as shown in the X-ray radiographs in Fig. 11 and photographs in Fig. 12. This is somewhat surprising since a net-tension mode was expected for the narrow specimens due to the increased tensile stress concentrations at the hole edge at $\theta = 90^{\circ}$ with decreased width. That net-tension mode has been observed for brittle T300/5208 CFRP material system for $w/d = 3$ in [1].

Typical load–displacement curves of the Q2 and Q3 specimens are shown in Figs. 13 and 14, respectively, as a function of the w/d for a constant ratio of $e/d = 3$. The wider specimens (Q2W and Q3W) exhibited bearing failure modes as expected. The narrow specimens for both lay-ups (Q2N and Q3N) experienced mixed-mode failure which resulted in a sudden load drop and reduced

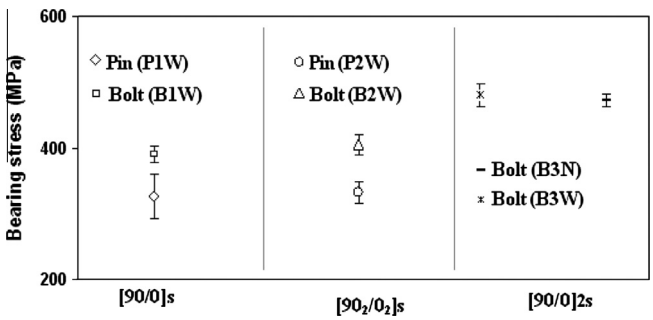

Fig. 8. Bearing stress of the cross-ply specimens at failure.

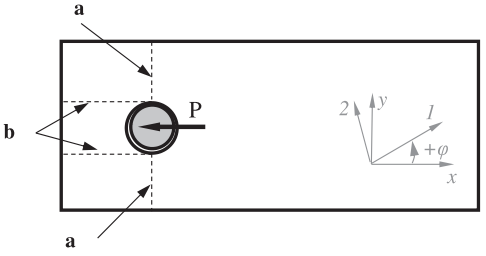

Fig. 9. Subcritical in-plane damage planes observed in cross-ply lay-ups: (a) transverse matrix cracking planes in 90° layers, and (b) axial split planes in 0° layers.

Table 2
Quasi-isotropic finger-tight bolted joint specimen test parameters.

Laminate	Specimen code	w/d	e/d
$[+45°/0°/-45°/90°]_s$	Q1W	6	3
	Q1N	3	3
$[90°/+45°/-45°/0°]_s$	Q2W	6	3
	Q2N	3	3
$[0°/90°/+45°/-45°]_s$	Q3W	6	3
	Q3N	3	3

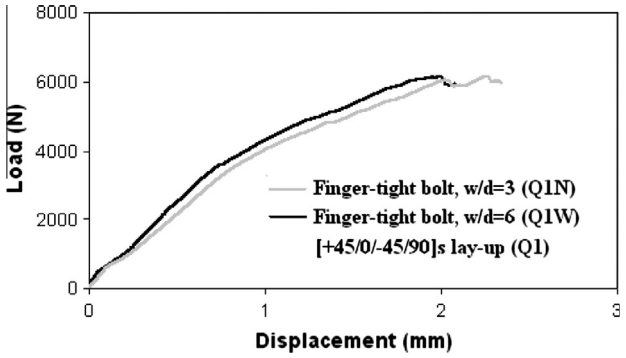

Fig. 10. Typical load–displacement curves of finger-tight bolted joints in $[45°/0°/-45°/90°]_s$ lay-up as a function of w/d (e/d = 3).

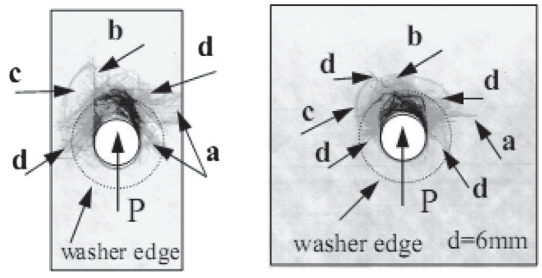

Fig. 11. Damage in bolted $[45°/0°/-45°/90°]_s$ lay-up at ultimate load: (a) transverse matrix cracks, (b) 0° axial splits, (c) delamination and (d) ±45 axial splits.

strength values, see Figs. 15–17. Mixed-mode failures generally include transverse tensile cracks in 90° layers, axial splits in 0° and ±45° layers and extensive delamination between all the interfaces.

Therefore, it is clear that the modes of failure are not only a function of the specimen geometry. The high strength of the fibres (HTS40) and high toughness of the resin matrix (977-2) used in the current material system is the main reason for change in the mode of failure. In comparison, HTS40 fibres and the similarly widely used T300 fibres have tensile strengths of 4275 MPa and 3530 MPa, respectively.

Accordingly, the high stress concentration developed at the hole edge (at $\theta = 90°$) may not reach the strength value of the fibres in the present specimens. This results in some other matrix dominated failure modes with increased bolt displacement. Smith and Pascoe [22] have reported similar mixed-mode of failures for the XAS/914 CFRP material system, which has high tensile strength fibres that are comparable to those of the currently discussed system.

However, the presence of high strength fibres in the current material system alone does not explain why narrow specimens of different lay-ups failed in different modes (Q1N failed in bearing

Fig. 12. Photographs of failed bolted joint specimens in $[45°/0°/-45°/90]_s$ lay-up as a function of w/d (e/d = 3).

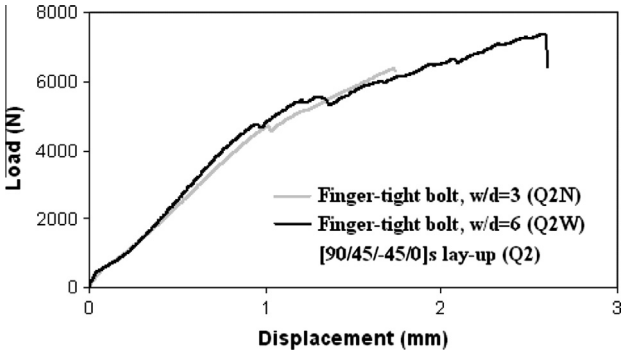

Fig. 13. Typical load–displacement curves of finger-tight bolted joints in $[90°/45°/-45°/0°]_s$ lay-up as a function of w/d (e/d = 3).

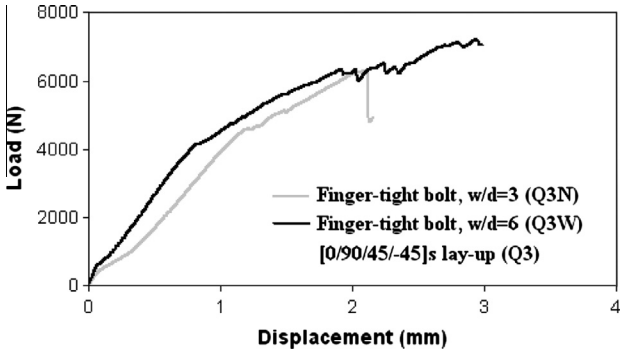

Fig. 14. Typical load–displacement curves of finger-tight bolted joints in $[0°/90°/45°/-45°]_s$ lay-up as a function of w/d (e/d = 3).

mode). A possible explanation may be the dependency of thermal stresses induced by the production of the CFRP laminates on the stacking sequence. It has been shown that the interlaminar normal stresses (ILNSs) developed during the cool-down process after curing may cause important changes in the local failure mechanisms of bolted joints in quasi-isotropic CFRP laminates [27] and those local changes may result in global changes to the failure mode [4].

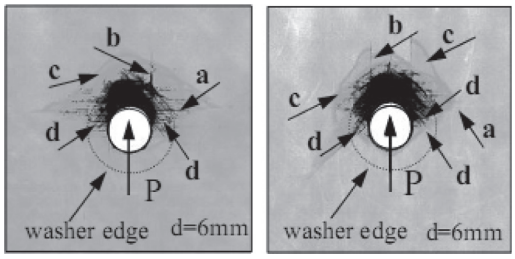

(i) $[90^{\circ}/45^{\circ}/-45^{\circ}/0^{\circ}]_s$, e/d=3, w/d=6

(ii) $[0^{\circ}/90^{\circ}/45^{\circ}/-45^{\circ}]_s$, e/d=3, w/d=6

Fig. 15. Damage in bolted quasi-isotropic lay-ups at ultimate load: (a) transverse matrix cracks, (b) 0° axial splits, (c) delamination and (d) ±45 axial splits.

Although it has been shown that the shear stress distribution is not affected by the width of the specimen for quasi-isotropic laminates [28], a specific layer should be considered separate from its surrounding layers due to interlaminar cracking (delamination). When re-examined as separate layers, the width effect may become more important with respect to the observed mixed-mode of failure.

The bearing stresses at failure (average of three specimens) are given in Fig. 18. The Q2W specimens show approximately 14% and 5.6% increased strength over Q1W and Q3W specimens, respectively. The same trend was observed for GFRP specimens by Quinn and Matthews [29] which was associated with the 90° layers placed at or close to the outer surface. According to classical lamination theory (CLT) [30], those 90° layers produce compressive ILNS at the hole boundary and increase the strength of the joint.

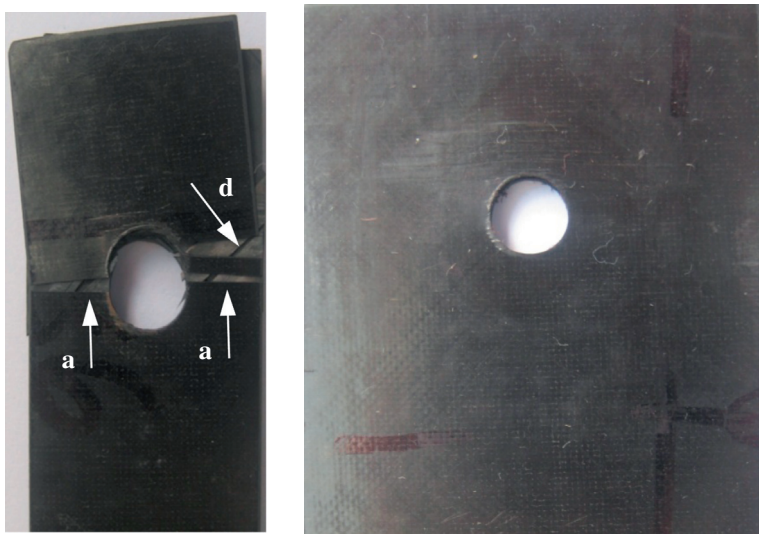

(i) $[90^{\circ}/45^{\circ}/-45^{\circ}/0^{\circ}]_s$, e/d=3, w/d=3
Mixed-mode failure

(ii) $[90^{\circ}/45^{\circ}/-45^{\circ}/0^{\circ}]_s$, e/d=3, w/d=6
Bearing failure

Fig. 16. Photographs of failed bolted joint specimens in $[90°/45°/-45°/0]_s$ lay-up as a function of w/d ($e/d = 3$): (a) transverse matrix cracks, and (d) ±45 axial splits.

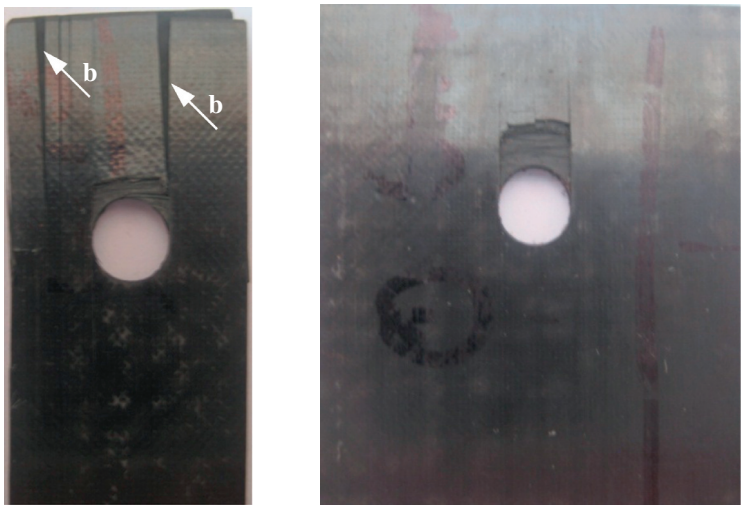

(i) $[0^{\circ}/90^{\circ}/45^{\circ}/-45^{\circ}]_s$, e/d=3, w/d=3
Mixed-mode failure

(ii) $[0^{\circ}/90^{\circ}/45^{\circ}/-45^{\circ}]_s$, e/d=3, w/d=6
Bearing failure

Fig. 17. Photographs of failed bolted joint specimens in $[0°/90°/45°/-45°]_s$ lay-up as a function of w/d ($e/d = 3$): (b) 0° axial splits.

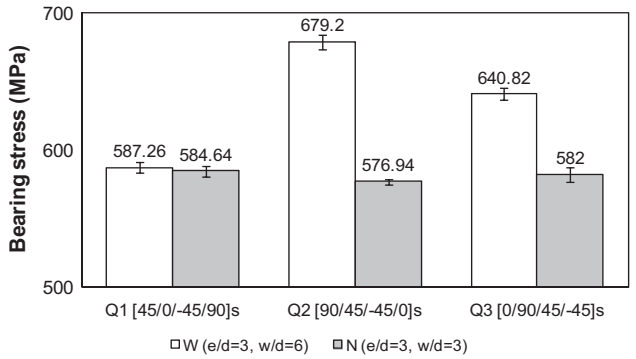

Fig. 18. Bearing stresses of quasi-isotropic specimens at failure.

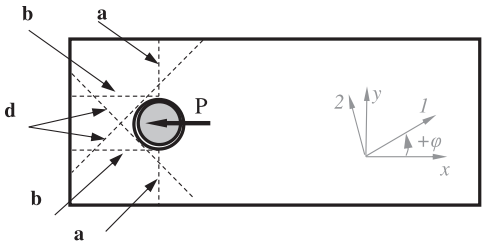

Fig. 19. Subcritical in-plane damage planes observed in quasi-isotropic lay-ups: (a) transverse matrix cracking planes in 90° layers, (b) axial split planes in 0° layers, and (d) axial split planes in ±45° layers.

The difference in strength of the Q1W and Q1N specimens is insignificant. This is because of the identical bearing mode of failure observed for both specimens. The lower strengths of the Q2N and Q3N specimens in contrast to their wider counterparts Q2W and Q3W is associated to their sudden mixed-mode failures.

The schematic of the subcritical in-plane damage planes observed from the X-ray radiographs of the quasi-isotropic lay-ups is given in Fig. 19. The transverse matrix crack and the axial split planes were determined as for the cross-ply lay-ups explained earlier. Axial split planes within the ±45° layers were located tangent to hole boundary at $\theta = \pm 45^\circ$ across the width of the specimen as observed from the failed specimens.

4. Conclusions

Single fastener double-shear tensile tests of various joint geometries were conducted for a wide range of cross-ply and quasi-isotropic lay-ups of HTS40/977-2 CFRP material system which provide a considerable strength database. The X-ray radiography technique was used to define the subcritical damage locations since no related study was found in the literature. These subcritical damage locations can be incorporated into three-dimensional finite element models in order to develop physically based strength prediction methods.

It is shown that the sublaminate-level scaled $[90^\circ/0^\circ]_{2s}$ and ply-level scaled $[90^\circ_2/0^\circ_2]_s$ bolted joint specimens had entirely different strengths due to the different subcritical damage accumulations. Strength differences up to 14% were observed for the quasi-isotropic bolted joint specimens that failed in bearing mode. It is attributed to the location of the 90° layers that modifies the ILNS around the hole boundary. The lower strength of the Q2N and Q3N specimens are related to their sudden mixed-mode of failure. The high strength fibres and toughened epoxy resin in the current material system are one of the reasons for that mixed-mode of failure. The interlaminar cracks (or other subcritical damage mechanisms) mainly driven by Mode-II shear stress components in bolted joints in which the cohesive zone length is significantly longer than that of Mode-I. This means that delamination damage can initiate at lower load levels but, its propagation requires considerable additional load. A strength based onset criterion thus is not sufficient for actual response prediction. Consequently, a discrete definition of each subcritical damage plane is necessary for accurate strength predictions in bolted joints which can be accomplished by using cohesive zone elements (CZEs). This modelling approach will be attempted by the authors in near future work.

Acknowledgment

The authors wish to acknowledge the Turkish Council of Higher Education (YÖK) for the PhD scholarship awarded to Dr. A. Ataş.

References

[1] Hart-Smith LJ. Bolted joints in graphite–epoxy composites. Douglas Aircraft Company, NASA Langley Report NASA CR-144899; 1976.
[2] Hart-Smith LJ. Mechanically-fastened joints for advanced composites – phenomenological considerations and simple analyses. In: Lenoe EM, Oplinger DW, Burke JJ, editors. Fibrous composites in structural design. New York: Plenum Press; 1980. p. 543–74.
[3] Hart-Smith LJ. Design and analysis of bolted and riveted joints in fibrous composite structures. In: Tong L, Soutis C, editors. Recent advances in structural joints and repairs for composite materials. Kluwer Academic Publishers; 2003. p. 211–54.
[4] Atas A. Strength prediction of mechanical joints in composite laminates based on subcritical damage modelling. Sheffield, UK: The University of Sheffield; 2012.
[5] Jumahat A, Soutis C, Jones FR, Hodzic A. Fracture mechanisms and failure analysis of carbon fibre/toughened epoxy composites subjected to compressive loading. Compos Struct 2010;92(2):295–305.
[6] ASTM D 5961/D 5961M–01. Standard test method for bearing response of polymer matrix composite laminates. United States; 2001.
[7] Atas A, Mohamed G, Soutis C. Modelling delamination onset and growth in pin loaded composite laminates. Compos Sci Technol 2012;72(10):1096–101.
[8] Atas A, Mohamed G, Soutis C. Progressive failure analysis of bolted joints in composite laminates plastics, rubber and composites. Macromol Eng 2012;41(4–5):209–14.
[9] Atas A, Arslan N, Sen F. Failure analysis of laminated composite plates with two parallel pin-loaded holes. J Reinf Plas Compos 2009;28(10):1265–76.
[10] Atas A, Demircioglu TK, Arslan N, Soutis C. Progressive failure analysis of bolted carbon fiber/epoxy composite plates. In: Proceedings of 2 national design, manufacturing and analysis congress, Balikesir, Turkey, conference 11–12 November, conference 2010. p. 138–48.
[11] Atas A, Sen F, Arslan N. Investigation of mechanical behaviours of parallel pin-loaded composite plates under static loading. Celal Bayar Univ J Tech Sci 2009;2(12):83–96.
[12] Chang FK, Qing XL. Strength determination of mechanical fastened joints. In: Tong L, Soutis C, editors. Recent advances in structural joints and repairs for composite materials. The Netherlands: Kluwer Academic Publishers; 2003. p. 101–40.
[13] Matthews FL, Camanho PP. Stresses in mechanical fastened joints. In: Tong L, Soutis C, editors. Recent advances in structural joints and repairs for composite materials. The Netherlands: Kluwer Academic Publishers; 2003. p. 67–100.
[14] Camanho PP, Matthews FL. A progressive damage model for mechanically fastened joints in composite laminates. J Compos Mater 1999;33(24):2248–80.
[15] Soutis C, Fleck NA. Static compression failure of carbon–fiber T800/924c composite plate with a single hole. J Compos Mater 1990;24(5):536–58.
[16] Soutis C, Fleck NA, Curtis PT. Hole hole interaction in carbon–fiber epoxy laminates under uniaxial compression. Composites 1991;22(1):31–8.
[17] Soutis C, Lee J. Scaling effects in notched carbon fibre/epoxy composites loaded in compression. J Mater Sci 2008;43(20):6593–8.
[18] Lee J, Soutis C. Measuring the notched compressive strength of composite laminates: specimen size effects. Compos Sci Technol 2008;68(12):2359–66.
[19] Lee J, Soutis C. A study on the compressive strength of thick carbon fibre–epoxy laminates. Compos Sci Technol 2007;67(10):2015–26.
[20] Lee J, Soutis C. Thickness effect on the compressive strength of T800/924C carbon fibre–epoxy laminates. Compos Part a – Appl Sci Manuf 2005;36(2):213–27.
[21] Kortschot MT, Beaumont PWR. Damage mechanics of composite-materials. 1. Measurements of damage and strength. Compos Sci Technol 1990;39(4):289–301.
[22] Smith PA, Pascoe KJ. Behaviour of bolted joints in [0/90]ns laminates. Cambridge University, CUED/C-mat./TR.121; 1985.
[23] Collings TA. On the bearing strengths of CFRP laminates. Composites 1982;13(3):241–52.
[24] Soutis C. Measurement of the static compressive strength of carbon–fiber epoxy laminates. Compos Sci Technol 1991;42(4):373–92.

[25] Mandell JF, Wang SS, Mcgarry FJ. Extension of crack tip damage zones in fiber reinforced plastic laminates. J Compos Mater 1975;9:266–87.
[26] Wisnom MR, Chang FK. Modelling of splitting and delamination in notched cross-ply laminates. Compos Sci Technol 2000;60(15):2849–56.
[27] Smith PA, Pascoe KJ. The effect of stacking-sequence on the bearing strengths of quasi-isotropic composite laminates. Compos Struct 1986;6(1–3):1–20.
[28] Crews JH, Hong CS, Raju IS. Stress-concentration factors for finite orthotropic laminates with a pin-loaded hole. NASA Technical Paper 1862; 1981. p. 44.
[29] Quinn WJ, Matthews FL. Effect of stacking sequence on pin-bearing strength in glass-fiber reinforced plastic. J Compos Mater 1977;11:139–45.
[30] Jones RM. Mechanics of composite materials. 2nd ed. USA: Taylor&Francis; 1999.